SEMARAK ILMU PUBLISHING

Semarak Journal of Thermal-Fluid Engineering

Journal homepage:
https://semarakilmu.my/index.php/sjotfe/index
ISSN: 3030-6639

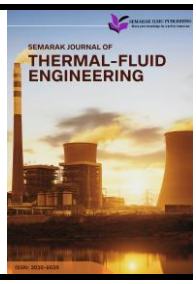

Simulation of Turbulent Flow in a Pipe with Multiple Internal Obstacles

Muhammad Afif Rifaie Aziz[1,*]

[1] Department of Mechanical Engineering, Fakulti Kejuruteraan Mekanikal dan Pembuatan, Universiti Tun Hussein Onn Malaysia, 86400 Batu Pahat, Johor, Malaysia

ARTICLE INFO

Article history:
Received 8 June 2025
Received in revised form 20 July 2025
Accepted 25 July 2025
Available online 29 September 2025

Keywords:
Turbulent flow; internal obstacles; pipe flow simulation; k–ω SST model; computational fluid dynamics

ABSTRACT

Turbulence in pipes and tubes is commonly observed in industrial systems, especially when internal obstructions cause flow disturbances. Understanding such flow behaviour is essential for enhancing system efficiency and reducing energy losses. This study aims to investigate turbulent fluid flow within different sections of a mechanical system using Computational Fluid Dynamics (CFD) simulations. The primary objective is to analyse how the fluid behaves under various configurations and to compare results across different scenarios to gain deeper insights into turbulent internal flow. In this simulation, the influence of internal obstacles on velocity and pressure distribution is explored. Two types of pipe geometries are considered, both containing square obstacles; however, their diameters differ to 1.5 cm and 3.0 cm respectively. Additionally, the obstacle sizes are proportionally scaled to match each pipe diameter. Three inlet velocities are used: 0.297 m/s, 0.397 m/s, and 0.497 m/s. These variations allow for the examination of how increasing flow intensity affects fluid characteristics and energy losses. The simulations are carried out using the k-ω turbulence model, which is appropriate for modelling incompressible turbulent flows. Meshes are generated with appropriate resolution and boundary conditions to ensure simulation accuracy. The results indicate that both the obstacle size and pipe diameter significantly influence the turbulence. Larger obstacles tend to increase turbulence intensity, while wider pipes facilitate smoother flow by reducing velocity gradients. Higher inlet velocities induce greater turbulence, emphasizing the role of internal geometry in shaping flow patterns. Velocity and pressure profiles are analysed and compared numerically across all cases. These findings suggest that optimizing obstacle shape and size, relative to pipe diameter and inlet velocity, can effectively control pressure drops and achieve desired flow characteristics.

1. Introduction

Turbulent flow through pipes is a widespread and critical phenomenon encountered in various engineering and industrial systems such as heat exchangers, water distribution systems, oil and gas pipelines, and chemical processing equipment. These systems often involve high Reynolds number flows, where turbulent behaviour dominates fluid transport and significantly influences performance

* *Corresponding author.*
E-mail address: muhammad.afif.rifaie@gmail.com

https://doi.org/10.37934/sjotfe.6.1.2841a

outcomes such as pressure loss and heat transfer efficiency [1,2]. Turbulence is characterized by chaotic, irregular fluctuations of velocity and pressure, which enhance mixing and convective transport but also lead to increased drag and energy loss. Kalpakli *et al*., [3] highlighted that the chaotic and stochastic motion of turbulent flows contributes to rapid mixing and high convective heat transfer rates but also results in large pressure drops compared to laminar flows.

In many engineering applications, the internal surfaces of pipes are intentionally modified using geometric features such as baffles, twisted tapes, and ribs to manipulate the flow field and improve system performance. These internal obstacles are introduced primarily to control flow separation, enhance heat transfer, and promote mixing. However, while these modifications serve to improve thermal efficiency, they also introduce complex fluid behaviours such as flow separation, recirculation zones, and the formation of secondary structures like vortices, all of which can increase pressure losses and reduce overall system performance [4,5]. For instance, Dean vortices that caused by centrifugal forces acting on the fluid in curved or obstructed paths which are commonly observed in such configurations and have a significant impact on the local velocity and pressure fields [5,6].

Several studies have focused on the effects of internal obstacles in modifying pipe flow behaviour. These include twisted tape inserts [7-9], helical and wing-type baffles [10,11], repeated obstruction ribs [12], and triangular perforations [9,13]. These design modifications induce swirling flows and secondary vortices that disrupt the boundary layer, thereby increasing radial mixing and the local turbulence level. Such changes typically enhance thermal performance, but at the cost of increased friction and pressure drop. Shukla *et al.,* [7], reported that twisted tapes can improve the temperature difference across a pipe by up to 50.52%, while Kalpakli *et al.,* [10], demonstrated that inclined twisted baffles achieved a thermal performance factor of 1.98 under optimized conditions. Similarly, Paul *et al.,* [14] and Youcef *et al.,* [15] reported substantial improvements in heat transfer for pipes equipped with novel baffle and rib configurations.

Although experimental studies have played a significant role in analysing turbulent flow characteristics, traditional laboratory techniques like Particle Image Velocimetry (PIV) and Laser Doppler Anemometry (LDA) face several limitations. These include challenges in accessing internal pipe geometries, high operational costs, and limited spatial resolution [16,17]. Consequently, Computational Fluid Dynamics (CFD) has emerged as a powerful tool for simulating and analysing complex flow behaviour in geometrically modified systems. CFD allows for a detailed and non-intrusive examination of flow variables such as velocity, pressure, and turbulence, offering high spatial and temporal resolution at relatively lower costs compared to physical experiments [18].

In CFD, the flow field is resolved by numerically solving the fundamental governing equations—the continuity and Navier–Stokes equations using the finite volume method. These equations account for mass and momentum conservation and are solved iteratively across a discretized computational domain that replicates the geometry of the actual system [18]. To model turbulence, which introduces a wide range of fluctuating scales, suitable turbulence models must be employed. Among the various models available, the Reynolds-Averaged Navier–Stokes (RANS) approaches—such as the standard k–ε, realizable k–ε, RNG k–ε, and k–ω SST models are widely used due to their computational efficiency and adequate accuracy for steady-state simulations [1,4,19]. While Large Eddy Simulation (LES) methods offer superior resolution of transient turbulent structures, they are generally limited to research applications due to high computational demands. Therefore, this study employs the k–ω SST model, which effectively captures flow separation and swirl effects common in geometries with internal obstacles.

The present study simulates turbulent water flow through a straight circular pipe with various internal obstacle configurations using ANSYS Fluent. Two distinct geometries are considered: geometry 1, with a diameter of 1.5 cm and length of 1 m, and Geometry 2, with a diameter of 3 cm

and the same length. Both geometries include four types of internal modifications twisted tape inserts, transverse baffles, repeating obstruction ribs, and triangular baffles. These geometries are analysed under three different inlet velocities (0.297 m/s, 0.397 m/s, and 0.497 m/s), yielding Reynolds numbers around 4,338 to ensure fully turbulent flow conditions. A grid independence test is performed for both geometries to ensure the accuracy and stability of the simulation results.

Simulation results reveal significant differences in flow behaviour based on geometry and inlet velocity. Flow separation and vortex generation are more prominent in pipes with tighter diameters (Geometry 1), leading to greater turbulence intensity and pressure drop. Twisted tape inserts were found to be most effective in generating strong swirling flows along the pipe's centreline, thereby enhancing mixing. In contrast, transverse baffles induced large separation zones downstream of each baffle, especially at higher inlet velocities. These recirculation zones increase turbulence but also contribute to energy losses. Geometry 2, with its larger cross-sectional area, showed more uniform flow distribution and lower turbulence intensities, allowing for smoother flow recovery and reduced pressure gradients [14,19,20].

Moreover, thermal enhancement factors, Nusselt number improvements, and pressure drop penalties associated with each configuration align with findings from past studies [11,13,15]. For example, twisted tape inserts with perforations achieved up to 20.8% improvement in heat transfer and reduced pressure drop by 27.7% [9], while ribs and fins demonstrated enhanced cooling effects in turbine blade applications [12].

In conclusion, this study offers a detailed CFD-based analysis of turbulent flow in pipes with multiple internal obstacles. The results underscore the importance of obstacle geometry, spacing, and pipe diameter in determining flow behaviour, pressure losses, and turbulence characteristics. The insights gained from this study are valuable for the design and optimization of fluid transport systems, heat exchangers, and gas turbine cooling passages, where efficient flow and thermal management are critical [7,10,11,19,21].

2. Methodology

Methodology describes the procedures and tools that are utilized to simulate turbulent flow in a pipe with internal obstacles of the multiple types. Four special configurations of the pipe with a twisted tape insert, the pipe with transverse baffles, the pipe with repeating obstruction ribs, the pipe with triangular baffles is investigated in the simulation. Here, the effect that different obstacle shapes and placements have on the flow behaviour, namely velocity profile, pressure drop, and turbulent intensity will be the focus of the simulation. The simulations are performed using Computational Fluid Dynamics (CFD) techniques and appropriate turbulence models are used to appropriately resolve the complex flow behaviour. There are several stages which must be accomplished during an overall simulation: geometry creation, meshing, application of boundary conditions, solver configuration and analysis of results.

2.1 Geometry of the Pipe with Multiple Internal Obstacles

Two different pipe geometries are used in this study to examine the effects of obstacle size and scale on turbulent flow behaviour. The first geometry includes a straight circular pipe 1.5 cm in diameter and 1 m in length. Dimensions of the internal obstacles are calculated to fit proportionally within this pipe size and modelled: namely, twisted tape inserts, transverse baffles, repeating obstruction ribs, and triangular baffles. The second geometry is scaled up version of the first. It consists of a pipe of diameter 3 cm and length of 1 m. In keeping with the same proportional

arrangement, all internal obstacle dimensions in Geometry 2 are doubled compared to those in Geometry 1. This scaling approach then allows such a comparison of flow characteristics and turbulence effects across various pipe sizes, whilst maintaining geometric similarity. The geometry creation can be seen in the Figure 1 and Figure 2 for both Geometry 1 and Geometry 2.

Fig. 1. Side view of the geometry

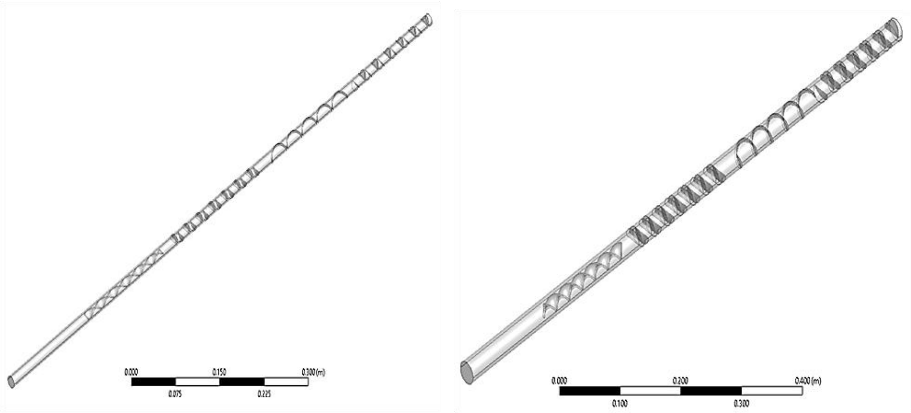

(a) (b)

Fig. 2. Geometry of pipe (a) Geometry 1 with diameter 1.5 cm (b) Geometry 2 with diameter 3 cm

2.2 Meshing

The mesh is of paramount importance in the CFD process since it is the one that directly influences the simulation accuracy and stability. In this work, ANSYS Meshing has been used to mesh that process. The tetrahedral mesh type is relied because of its capacity to perform well for irregularities such as twisted tape inserts, transverse baffles, blockage ribs, triangular baffles and so on; mesh refinement in areas near pipe surfaces as well as around the obstacles is done in order to assure the right flow features like boundary layer development and formation of vortices. This meshing approach yields a good compromise between computational cost and required level of detail for a good flow simulation. Figure 3 and Figure 4 below shows the meshing of the geometry 1 and geometry 2 at default element size which is 50.011 mm and number of nodes 24863 foe geometry 1 while 50.045 mm element size with 23885 number of nodes for the geometry 2.

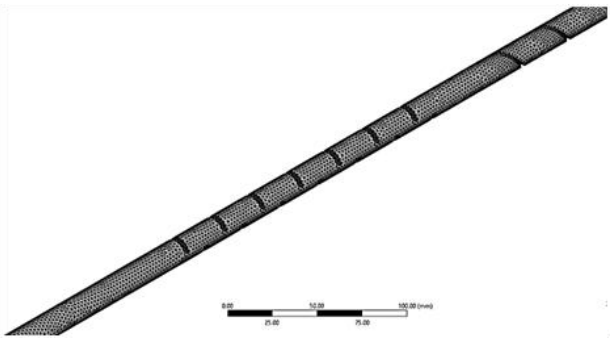

Fig. 3. Mesh of the geometry 1 at default setting

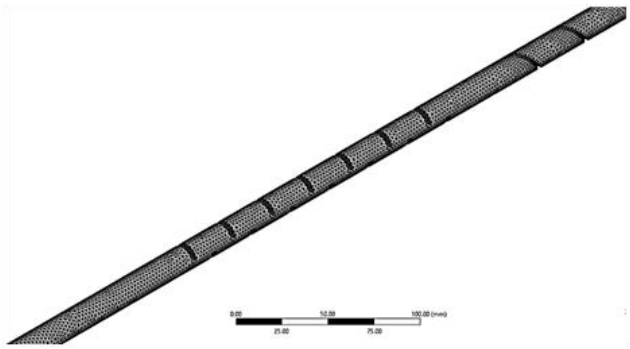

Fig. 4. Mesh of the geometry 2 at default setting

2.3 Governing Equation

The governing equations for the simulation of turbulent flow in this study are based on the fundamental equations of fluid dynamics such as continuity and Navier–Stokes. These equations are needed to describe the physical behaviour of fluid flow in a domain involving obstacles which produce complex flow patterns. The conservation of mass is ensured by continuity equation. It also says the rate at which mass enters a control volume equals the rate at which it leaves if there are no sources or sinks. For incompressible flow, fluid density is constant, and this is on important principle. On the other hand, the Navier–Stokes equations describe the time rate of change of the three momentum components of the fluid. The effects of pressure, viscous forces and body forces acting on the fluid are accounted for by them. These equations are vectors and are time dependent, thus modelling the steady and unsteady flow behaviour. In the turbulent regime, they become increasingly more complex because fluctuating velocity components are present and must be modelled with turbulence closure techniques. These equations, when taken together, represent the basis for the accurate description of fluid motion under a great variety of conditions, and this study solves them numerically in this form using the finite volume method in ANSYS Fluent. The continuity equation (mass conservation) is given by Eq. (1). While, the Navier-Stokes equations (momentum conservation) are expressed as in Eq. (2):

$$\frac{\partial \rho}{\partial t} + \nabla \cdot (\rho \vec{v}) = 0 \tag{1}$$

$$\rho \left(\frac{\partial \vec{v}}{\partial t} + \vec{v} \cdot \nabla \vec{v} \right) = -\nabla p + \mu \nabla^2 \vec{v} + \vec{F} \tag{2}$$

where ρ is fluid density, $\vec{v}$ is the velocity vector, p is pressure, μ is dynamic viscosity, $\vec{F}$ represent body forces (if any)

Under Model setup in ANSYS Fluent, k–ω turbulence model with the SST formulation is employed to capture all the effects of the turbulence imposed by the internal obstacles correctly. The SST variant of the k–ω model improves the standard model by adding a blending function that allows the k–ω model to transition between the wall and k–ε in the free stream. It is particularly suitable to handle flows characterized by separation, swirl and adverse pressure gradients, situations which are expected to materialize in this work, considering the presence of twisted tapes, ribs, and baffle.

2.4 Boundary Condition and Parameter Assumption

Given the same boundary conditions and assumptions of the parameter, the flow through the pipe with internal obstacle was simulated in this work. The velocity inlet boundary condition is applied at the inlet. Turbulence properties and the pressure drop are investigated as a function of inlet velocity at three different values. The selected velocities are:

i. 0.297 m/s
ii. 0.397 m/s
iii. 0.497 m/s

Inlet surface is applied uniformly for all the simulation cases. The pressure outlet boundary condition at the outlet with a gauge pressure of 0 Pa is set to allow fluid to leave the pipe domain freely with numerical stability. The outer pipe wall and the surfaces of any internal obstacles were both described using a condition that prevents the flow from being slipping due to its viscosity. The

wall area used for calculations was chosen by first selecting the internal perimeter of the pipe and all the front, back and side surfaces of the touching obstacles by name. As a result, the model could pinpoint how the growth of the boundary layer and wall-driven turbulence occurred in the flow. The diagram in Figure 5 below highlights the chosen areas for setting the boundary conditions (inlet, outlet and outer wall regions).

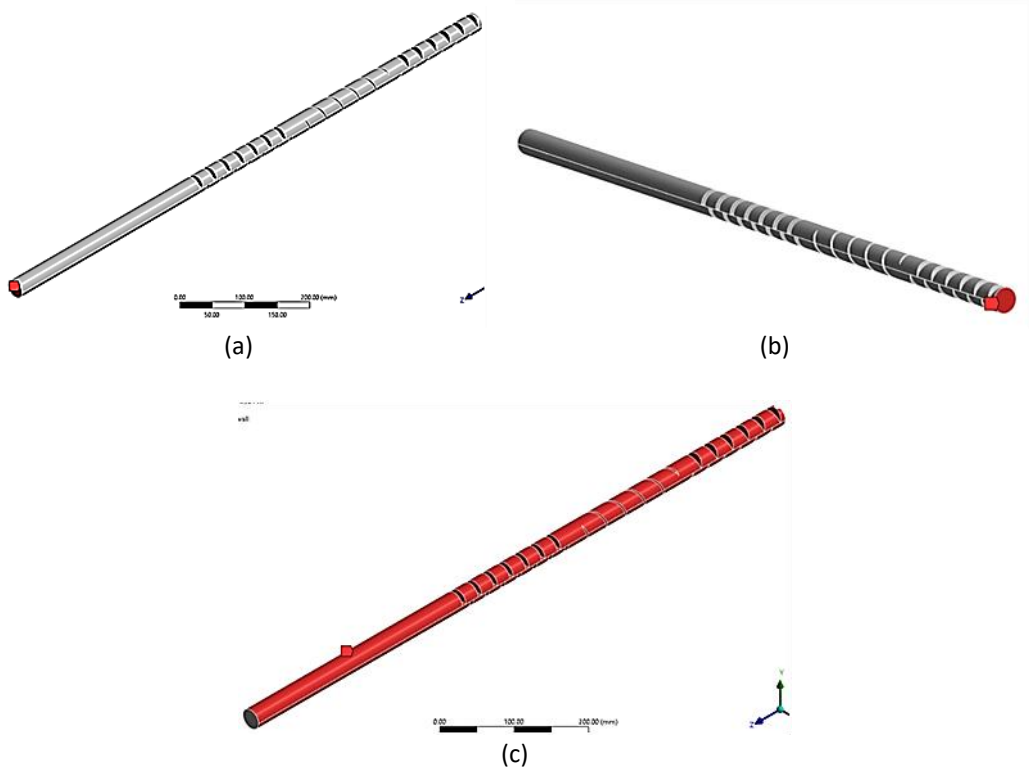

(a) (b)

(c)

Fig. 5. Chosen areas for setting boundary conditions (a) Inlet (b) Outlet (c) Outerwall

A working fluid of liquid water is selected from the standard Fluent material data base. It is assumed that density and viscosity of the fluid throughout the domain are constant. The surfacing of all the internal obstacles is assumed to be stationary with no slip condition (the velocity of the fluid with respect to the walls is zero at the boundary). This assumption is realistic for viscous behaviour of water interacting with solid surfaces. The pressure-velocity coupling is accomplished by using the SIMPLE (Semi-Implicit Method for Pressure-Linked Equations) algorithm for solution method. The iterative method is generally used in incompressible flow problems to obtain a convergent and a stable numerical solution.

2.5 Analysis

In the simulation, the post processing and analysis stage deals with analysing how turbulent flow behaves as it interacts with internal obstacles present in the pipe. The aim is to determine how the flow field, pressure drop, and turbulence characteristics depend on each one of the obstacle configurations and different inlet velocities. Among the analysis one of the key aspects is that the flow separation observed in the regions in which the geometry changes abruptly, for instance, downstream of baffles, ribs, and twisted tapes. Velocity contours, vector and streamlines are used to visualize the presence and extent of flow separation in the form of zones of recirculation with low momentum in the flow. Secondary flow structures including Dean vortices that typically develop in

curved and obstructed flow paths are also examined. The role of these structures in improvement of mixing and turbulence of the flow, especially in the repeated obstacle configuration, is analysed. Each internal structure is also studied in terms of the induced resistance to pressure distribution along the pipe. The energy losses are quantified using pressure plots and pressure drop values between the inlet and outlet due to different shapes and flow rates.

Furthermore, velocity profiles are extracted at different cross sections on the pipe to assess the uniformity and the distortion of the flow. The profiles give some insight into the development of boundary layers and flow acceleration or deceleration near the obstacles. This is complemented by the evaluation of the turbulence intensity, which is intended for understanding the local fluctuation of velocity and the scale of turbulence provided by each configuration. By combining the results from the two analyses, one can obtain a complete picture of how internal obstacles limit the flow behaviour in turbulent pipe systems and how each design compares in terms of hydraulic performance.

3. Results

The two geometries which are considered are geometry 1 which has a diameter of 1.5 cm and a length of 1m and geometry 2 which has diameter of 3 cm and a length of 1 m. There are four types of internal flow disturbing elements in each geometry including twisted tape inserts, transverse baffles, repeating obstruction ribs and triangular baffles. To investigate the effect of inlet velocity, the inlet velocity is computed at three different values, 0.297 m/s, 0.397 m/s and 0.497 m/s. For both geometries, these conditions are tested on all obstacle configurations. The results are compared for each geometry to the following the flow characteristics across the inlet velocities. Flow separation Secondary flow structures (such as vortex formation) pressure and velocity distributions Turbulence intensity Thus, this comparison provides insight regarding how increase of flow rate impacts the formation and behaviour of turbulent structures in terms of obstacle shape and pipe size.

3.1 Flow Separation and Secondary flow (Dean Vortices)

One of the prime features associated with the turbulent flow is flow separation, and it is frequently encountered because of the obstacles, which induce abrupt changes in the flow direction. The transverse baffle is identified to be the flow separation configuration that manifests the clearest separation effect against other obstacle types and is the primary subject of this study. the presence of transverse baffles results in rather large separation zones immediately downstream of each baffle, and the separation is separated more for geometry 2 (3 cm diameter) than for geometry 1 (1.5 cm diameter). These zones are recirculating regions of the flow detached from pipe surface because of the occurrence of sudden blockage and causing of adverse pressure gradient. Figure 6 shows the flow separation of geometry 1 with different velocity while Figure 7 shows the flow separation of geometry 2 with different velocity.

The flow separation is relatively mild at 0.297 m/s. Each baffle has small and symmetrical vortices behind that suggest moderate recirculation zones, with minimal disruption of the main flow. By increasing the velocity up to 0.397 m/s, there is more strong flow separation behind each baffle, more distinct Vortex cores and further downstream reattachment points. Splashing due to this separation is much more intense at the highest velocity, 0.497 m/s. The vortices grow larger and more chaotic and velocity vectors show stronger swirling motion and backflow intensity. With increasing flow, the flow becomes ever more unsteady and the extent of the recirculation zones in the downstream regions increases.

For Geometry 2, because of its larger diameter, tends to show wider but narrower separation zones. The increased cross section provides increased space for the separated flow to separate and reattach. However, Geometry 1 tighter confines the flow; at higher velocities, it improves recirculation. This analysis verifies that velocity increases do indeed increase flow separation intensity in confined geometries and that pipe size and geometric obstacle design determine the nature of the pressure losses and the overall flow stability.

In addition to separation, the interaction between the separated flow and the pipe walls gives birth to secondary flow structures such as Dean vortices. The vortices are spiral-like motion patterns that increase the mixing in the pipe. In geometry 1 the vortices grow more strongly and chaotically as the velocity increases, whereas in geometry 2 with the larger box the vortices retain their young and persistent character. Whereas in geometry 2 the larger diameter permits broader formation of the vortices with less intense one.

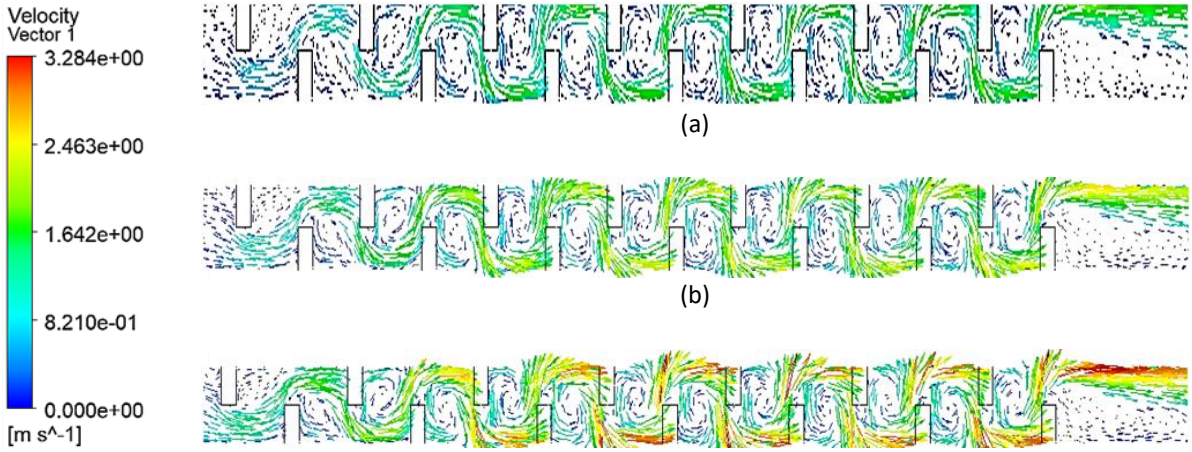

Fig. 6. Vector of velocity of geometry 1 (a) Velocity = 0.297m/s (b) Velocity = 0.397m/s (c) Velocity = 0.497m/s

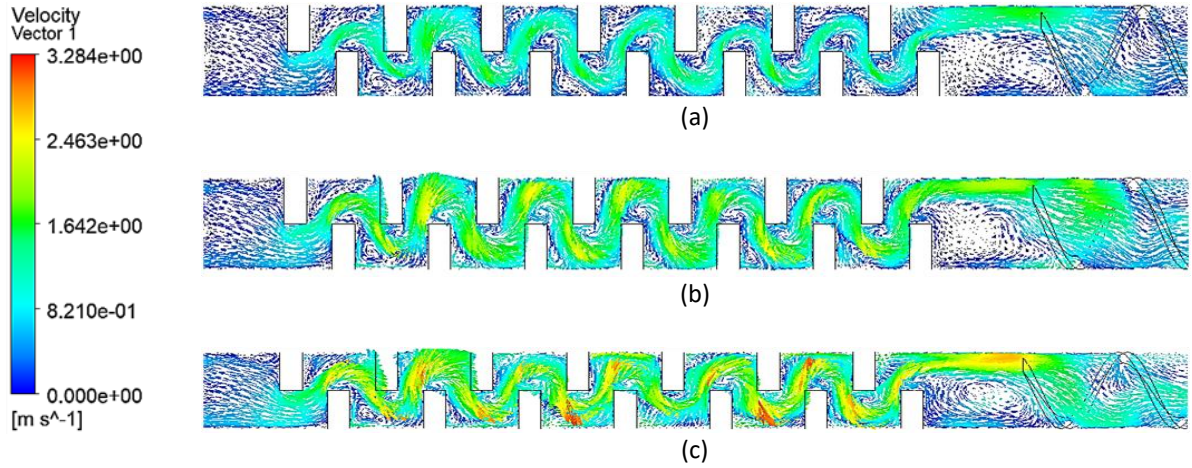

Fig. 7. Vector of velocity of geometry 2 (a) Velocity = 0.297 m/s (b) Velocity = 0.397 m/s (c) Velocity = 0.497 m/s

3.2 Pressure and Velocity Distribution

In the presence of the internal obstacles, the distribution of pressure and velocity in the pipe has important role in explanation of the turbulent flow behaviour. For instance, with this study, we

examined both parameters over three inlet velocities (0.297 m/s, 0.397 m/s, and 0.497 m/s) for geometries 1 and 2, and we showed how different obstacle positions affect the fluid dynamics.

3.2.1 Pressure distribution

The pressure difference across geometry 1 is less than in geometry 2, because the latter's obstacles are double the size and follow the same scaling. Because a substantial amount of fluid is severely constricted into the region, both models have high pressure. However, geometry 2 sees a markedly higher rise in the pressure. This is because its circle cross-section and the larger, flat area of obstacles offer more resistance to the water passing through the pipe. In the area with obstacles, pressure is gradually lower on each upright wall and there are clear signs of separated flow and recirculation in these sections. In geometry 2, the increased velocity results in larger forces being pushed down into the water which lasts for a longer period.

In outlet section, geometry 1 achieves a less steep pressure decline and more consistency, in contrary, geometry 2 has high-pressure zones in the immediate vicinity of the final structures. As the velocity increases to 0.497 m/s, pressure at the upstream areas rises and pressure at the downstream end falls for both pipelines. All things considered, the primary reason geometry 1 has less resistance to water movement is due to its hydrodynamic efficiency and lower pressure losses. Geometry 2 is often picked for use cases that benefit from more mixing or disturbance. Figure 8 and Figure 9 shows the contour of pressure distribution for both geometry 1 and 2 at different velocities inlet.

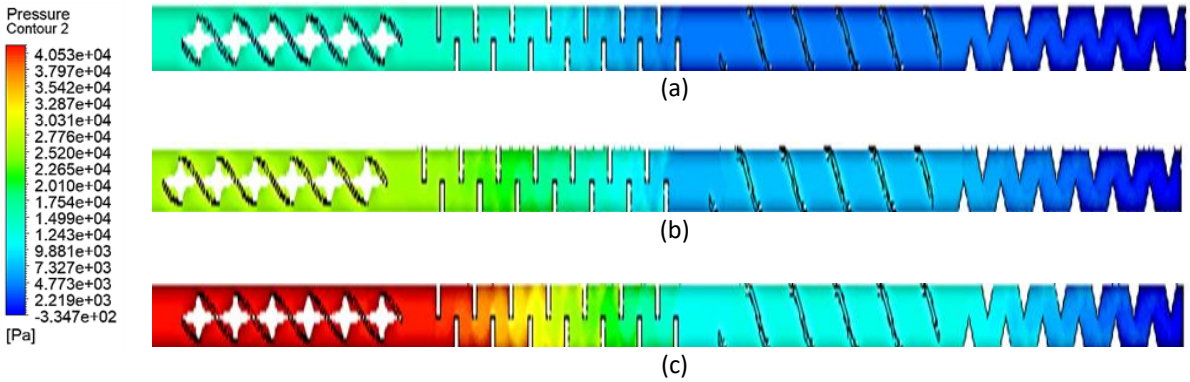

Fig. 8. Pressure distribution of geometry 1 (a) Velocity = 0.297 m/s (b) Velocity = 0.397 m/s (c) Velocity = 0.497 m/s

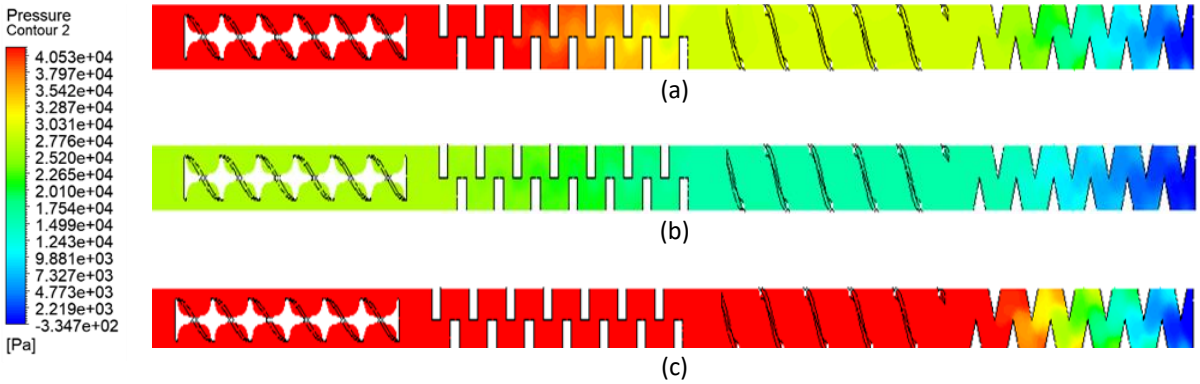

Fig. 9. Pressure distribution of geometry 2 (a) Velocity = 0.297 m/s (b) Velocity = 0.397 m/s (c) Velocity = 0.497 m/s

3.2.2 Velocity distribution

To understand how the flow progresses after interacting with the obstacles, velocity distribution was investigated along the z axis (the pipe length) as well as across different cross sections of the pipe. The velocity profile was smooth with moderate deviation near the obstacles, and early boundary layer growing, and distortion velocity were observed at 0.297 m/s. The flow was more disturbed with the appearance of localized accelerations and decelerations especially at separation regions and recirculating zones; it proceeded at a speed of 0.397 m/s. The velocity distribution showed clear evidence of flow asymmetry, strong swirling motion, and high turbulence in the wall regions and in the wake of the obstacles at the velocity of 0.497 m/s.

Both geometries demonstrated no-slip boundary conditions in which the core flow was faster than regions near the wall. Nevertheless, sharper velocity gradients and stronger wall interaction with the flow were found in Geometry 1, which had narrower diameter and greater interaction of the obstacles with the flow. It is found that both inlet velocity and pipe geometry play critical roles in designing and predicting real world application like heat exchangers and fluid transport systems with the results of this analysis confirming that both are influencing the internal flow characteristics, performance, and the design considerations. Figure 10 and Figure 11 show the velocity contour of geometry 1 and geometry 2.

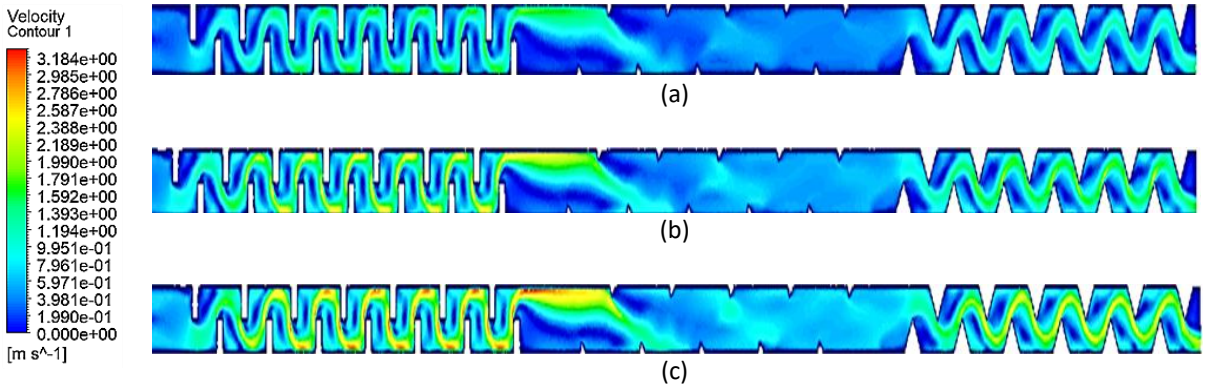

Fig. 10. Velocity distribution of geometry 1 (a) Velocity = 0.297 m/s (b) Velocity = 0.397 m/s (c) Velocity = 0.497 m/s

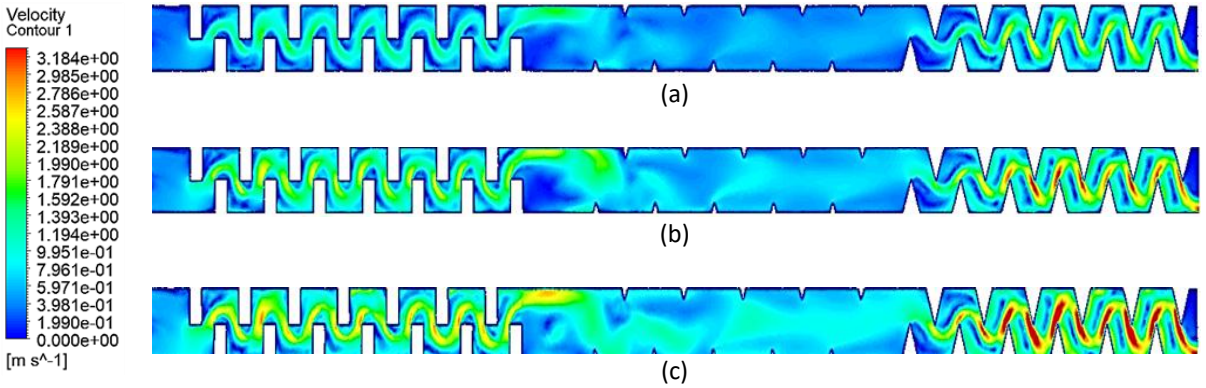

Fig. 11. Velocity distribution of geometry 1 (a) Velocity = 0.297 m/s (b) Velocity = 0.397 m/s (c) Velocity = 0.497 m/s

3.3 Turbulent Kinetic Energy

Figure 12 and Figure 13 help show how the turbulence in each geometry changes as the velocity of the inlet flow increases compared to geometry 1. In geometry 1, since the pipe diameter (1.5 cm) and obstacles are small, the flow usually remains calm and only has moderate turbulence in areas where the obstacles are located. With no wind, there is almost no turbulence and while the speed increases slightly, most turbulence still concentrates near the sides of the obstacle. However, objects in geometry 2 (3.0 cm diameter) show a much greater reaction to turbulence, occurring at higher flow rates than in the other geometry. When the inlet velocity rises, you can see that the turbulence occurs over a greater area because of the strong red and yellow colours visible in the TKE maps. This means that the larger obstacle and wider cross-section in geometry 2 make it easier for differences in the flow to cause turbulence. Clearly, turbulence in geometry 2 is higher which is useful for situations that involve more mixing or heat exchange; in contrast, geometry 1 guarantees a smoother and less turbulent flow.

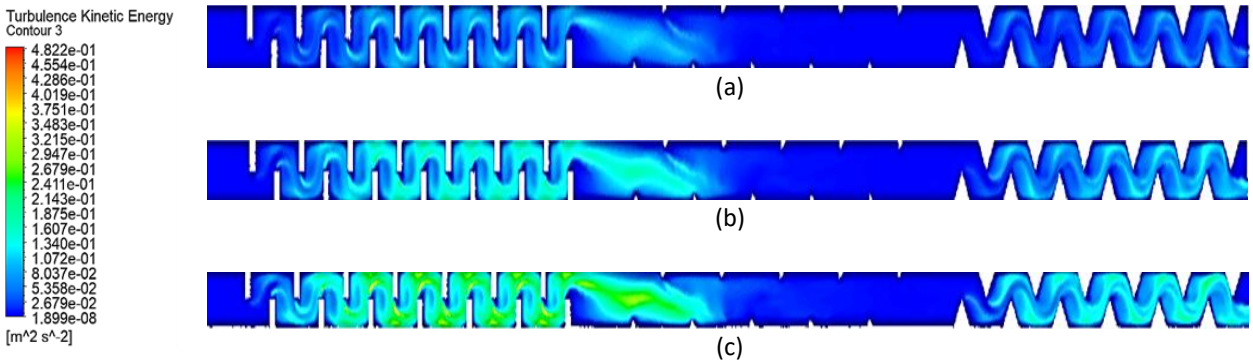

Fig. 12. Turbulent Intensity of geometry 1 (a) Velocity = 0.297 m/s (b) Velocity = 0.397 m/s (c) Velocity = 0.497 m/s

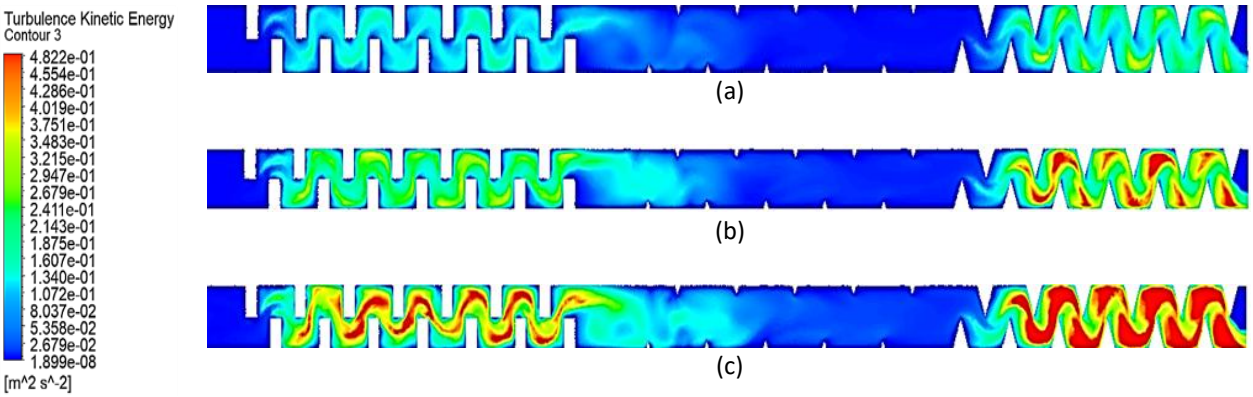

Fig. 13. Turbulent intensity of geometry 2 (a) Velocity = 0.297m/s (b) Velocity = 0.397m/s (c) Velocity = 0.497m/s

3.4 Grid Independent Test

To check whether the mesh resolution significantly affects the results of the simulation, a Grid Independence Test (GIT) is performed. It is very important for validating the accuracy and reliability of the numerical solution. It is done separately for the first geometry and the second one respectively. Six mesh configurations with different element sizes are tested for geometry 1. Same boundary and flow conditions are applied in each of the simulations and convergence is achieved in every case

before going on to the next test. Velocity distribution and pressure drop of key flow parameters are computed for the mesh sets and compared. Grid independence is assumed when the successive refinements in the mesh do not significantly change these parameters. Based on the results, a tetrahedral mesh with element size of 0.8 mm (368,518 nodes) is found to be the best mesh type for this geometry 1.

For geometry 2, the same is done. Finally, for the selected final mesh, we select the 270,223 nodes element size has 1.3 mm. Through this configuration, the resolution is adequate and the computational efficiency agreeable. The accurate meshes for both geometries are chosen as a compromise between accuracy and processing time, and they are good for the final simulation analysis. Figure 14 below shows the close-up of the meshing of the geometry 1 and geometry 2 at the best mesh selection by doing the grid independent test.

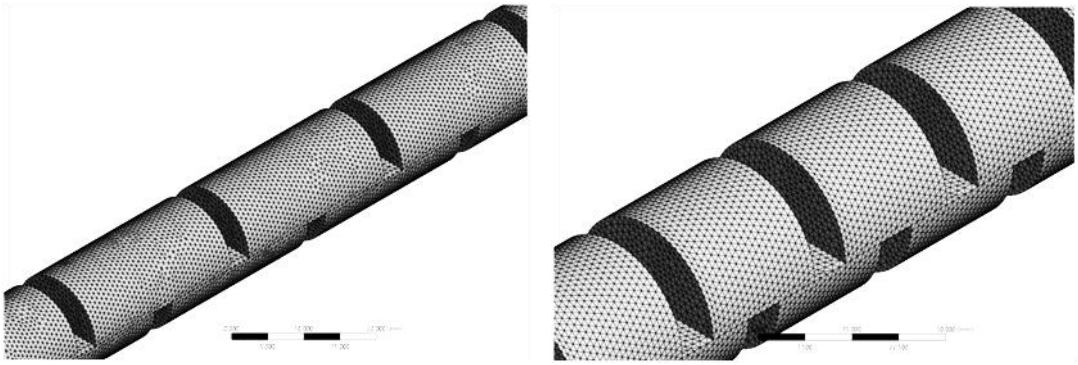

(a) (b)

Fig. 14. Close-up of the meshing (a) Geometry 1 (b) Geometry 2

The results from different mesh configurations are compared to clearly observe the differences in the mesh refinement effects by plotting a graph of velocity magnitude on z axis. Any deformation or nonconformity of the velocity distribution can be detected using this visualization owing to insufficient mesh resolution. The mesh is considered independent once velocity profiles between consecutive mesh levels have become negligible varying, in which case their configuration in the final simulations is taken. Figure 15 below shows the graph of grid independence test of geometry 1 and geometry 2.

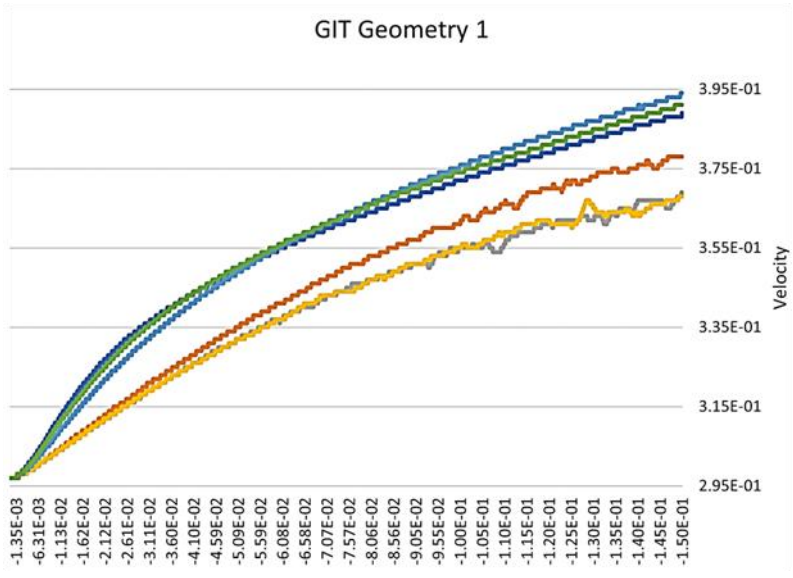

(a)

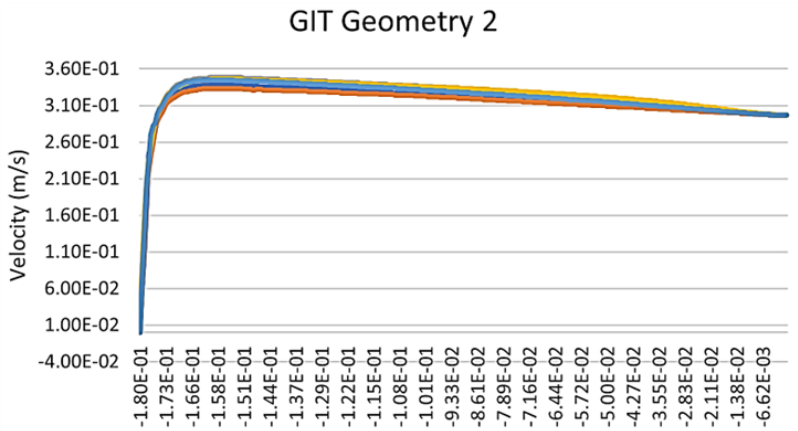

(b)

Fig. 15. (a) Graph of GIT geometry 1 (b) Graph of GIT geometry 2

4. Conclusions

In this study, the behaviour of turbulent pipe flow with internal obstacles such as twisted tape inserts, transverse baffles, repeating ribs, and triangular baffles was studied. For this, two geometries of different pipe diameters were analysed to investigate the effect of obstacle scaling and confinement of the flow. Computational Fluid Dynamics (CFD) tools with the k – ω SST turbulence model was used to simulate the flow separation effects, the secondary flow structures, the pressure and velocity distributions as well as the turbulence intensity over three different inlet velocities of 0.297 m/s, 0.397 m/s and 0.497 m/s. In conclusion, increased inlet velocity was found to lead to stronger turbulent behaviour, namely, more pronounced flow separation, higher velocity gradients, and enhanced secondary flows including dean vortices.

Due to tighter spacing of obstacles in geometry 1, it experienced greater turbulence, and more sharp velocity transitions and higher local turbulence intensity. By comparison, the more developed and distributed turbulence of geometry 2 was a result of the larger flow area. Flow separation was most pronounced with transverse baffles, and most swirling was produced by twisted tape inserts which also enhanced mixing and turbulence development along the centreline. Flow velocity also proved to be critical in assessing pressure drop and velocity deformation and the analysis showed that these values increased as the flow velocity increased. Results from the simulation are used in a conclusion which shows the significant influence of the geometry, placement, and the velocity of flow upon the turbulent behaviour in internal pipe flow. The insights are useful in optimizing heat exchanger, fluid transport device, and other engineering device designs that rely on controlled turbulence to improve performance.

References

[1] Arolla, Sunil K., and Olivier Desjardins. "Transport modeling of sedimenting particles in a turbulent pipe flow using Euler–Lagrange large eddy simulation." *International Journal of Multiphase Flow* 75 (2015): 1-11. https://doi.org/10.1016/j.ijmultiphaseflow.2015.04.010

[2] Diyoke, C., and U. Ngwaka. "CFD analysis of a fully developed turbulent flow in a pipe with a constriction and an obstacle." *International Journal of Engineering Research and Technology* 4 (2015): 2278-0181.

[3] Kalpakli, Athanasia. "Experimental study of turbulent flows through pipe bends." PhD diss., KTH Royal Institute of Technology, 2012. https://doi.org/10.1088/1742-6596/318/9/092023

[4] Yousfi, Sidi Mohammed, and Khaled Aliane. "Turbulent flow around obstacles: simulation and study with variable roughness." *International Journal of Heat and Technology* 39, no. 5 (2021): 1659-1666. https://doi.org/10.18280/ijht.390530

[5] Abreu, Leandra I., André VG Cavalieri, Philipp Schlatter, Ricardo Vinuesa, and Dan S. Henningson. "Spectral proper orthogonal decomposition and resolvent analysis of near-wall coherent structures in turbulent pipe flows." *Journal of Fluid Mechanics* 900 (2020): A11. https://doi.org/10.1017/jfm.2020.445

[6] Al-Obaidi, Ahmed Ramadhan, and Jassim Alhamid. "The effect of different twisted tape inserts configurations on fluid flow characteristics, pressure drop, thermo-hydraulic performance and heat transfer enhancement in the 3D circular tube." *International Journal of Ambient Energy* 44, no. 1 (2023): 57-72. https://doi.org/10.1080/01430750.2022.2091023

[7] Shukla, Anuj Kumar, Anupam Dewan, Rahul Salhotra, and Deepak Kumar Singh. "Thermal performance and turbulence modeling of combined multiple shell-pass shell and tube heat exchanger." *Journal of Thermal Science and Engineering Applications* 15, no. 7 (2023): 071006. https://doi.org/10.1115/1.4062240

[8] Cabello, Ruben, Alexandra Elena Plesu Popescu, Jordi Bonet-Ruiz, David Curcó Cantarell, and Joan Llorens. "Heat transfer in pipes with twisted tapes: CFD simulations and validation." *Computers & Chemical Engineering* 166 (2022): 107971. https://doi.org/10.1016/j.compchemeng.2022.107971

[9] Han, Je-Chin, and Hamn-Ching Chen. "Turbine blade internal cooling passages with rib turbulators." *Journal of Propulsion and Power* 22, no. 2 (2006): 226-248. https://doi.org/10.2514/1.12793

[10] Kalpakli, Athanasia, Ramis Örlü, Nils Tillmark, and P. Henrik Alfredsson. "Pulsatile turbulent flow through pipe bends at high Dean and Womersley numbers." In *Journal of Physics: Conference Series*, vol. 318, no. 9, p. 092023. IOP Publishing, 2011. https://doi.org/10.1088/1742-6596/318/9/092023

[11] Smithe, Stella. *Modeling of turbulent flow in pipe systems with compound bends*. Master diss., Florida Institute of Technology, 2023.

[12] Versteeg, Henk Kaarle. *An introduction to computational fluid dynamics the finite volume method, 2/E*. Pearson Education India, 2007.

[13] Kore, Sandeep Sadashiv, Manoj Kumar Chaudhary, Adhikrao Sarjerao Patil, and Vijay Dilip Kolate. "Computational study and enhancement of heat transfer rate by using inserts introduced in a heat exchanger." *Journal of Advanced Research in Fluid Mechanics and Thermal Sciences* 103, no. 1 (2023): 16-29. https://doi.org/10.37934/arfmts.103.1.1629

[14] Paul, Abhijit, Dipak Sen, and Ajoy Kumar Das. "3-D numerical study of the effect of Reynolds number and baffle angle on heat transfer and pressure drop of turbulent flow of air through rectangular duct of very small height." *Perspectives in Science* 8 (2016): 583-585. https://doi.org/10.1016/j.pisc.2016.06.027

[15] Youcef, Ahmed, Rachid Saim, Hakan F. Öztop, and Mohamed Ali. "Turbulent forced convection in a shell and tube heat exchanger equipped with novel design of wing baffles." *International Journal of Numerical Methods for Heat & Fluid Flow* 29, no. 6 (2019): 2103-2127. https://doi.org/10.1108/HFF-12-2018-0754

[16] Menni, Younes, Ahmed Azzi, Ali J. Chamkha, and Souad Harmand. "Effect of wall-mounted V-baffle position in a turbulent flow through a channel: Analysis of best configuration for optimal heat transfer." *International Journal of Numerical Methods for Heat & Fluid Flow* 29, no. 10 (2018): 3908-3937. https://doi.org/10.1108/HFF-06-2018-0270

[17] Al-Obaidi, Ahmed Ramadhan. "Investigation of the flow, pressure drop characteristics, and augmentation of heat performance in a 3D flow pipe based on different inserts of twisted tape configurations." *Heat Transfer* 50, no. 5 (2021): 5049-5079. https://doi.org/10.1002/htj.22115

[18] Vaisi, Ahmad, Rouhollah Moosavi, Moslem Lashkari, and M. Mohsen Soltani. "Experimental investigation of perforated twisted tapes turbulator on thermal performance in double pipe heat exchangers." *Chemical Engineering and Processing-Process Intensification* 154 (2020): 108028. https://doi.org/10.1016/j.cep.2020.108028

[19] Sarada, S. Naga, AV Sita Rama Raju, K. Kalyani Radha, and L. Shyam Sunder. "Enhancement of heat transfer using varying width twisted tape inserts." *International Journal of Engineering, Science and Technology* 2, no. 6 (2010). https://doi.org/10.4314/ijest.v2i6.63702

[20] Eiamsa-ard, Smith, and Varesa Chuwattanakul. "Visualization of heat transfer characteristics using thermochromic liquid crystal temperature measurements in channels with inclined and transverse twisted-baffles." *International Journal of Thermal Sciences* 153 (2020): 106358. https://doi.org/10.1016/j.ijthermalsci.2020.106358

[21] Turgut, Oguz, and Erkan Kizilirmak. "Effects of Reynolds number, baffle angle, and baffle distance on three-dimensional turbulent flow and heat transfer in a circular pipe." *Thermal Science* 19, no. 5 (2015): 1633-1648. https://doi.org/10.2298/TSCI121011045T